Practical Flapping Mechanisms for 20 cm-span Micro Air Vehicles

Lung-Jieh Yang[1], Balasubramanian Esakki[2], Udayagiri Chandrasekhar[3], Kuan-Cheng Hung[1], Chieh-Ming Cheng[1]

[1]Tamkang University, Department of Mechanical and Electromechanical Engineering, 151, Ying-Zhuan Rd., Tamsui, New Taipei City, 25137, TAIWAN

[2]Vel Tech University, Avadi, Chennai, INDIA

[3]ESCI-Institution of Engineers, Hyderabad, INDIA

Tel: +886-932-159193, Fax: +886-2-26209745; Email: Ljyang@mail.tku.edu.tw

ABSTRACT

In the body of research relevant to high-performance flapping micro air vehicles (MAV), development of light-weight, compact and energy-efficient flapping mechanisms occupies a position of primacy due to its direct impact on the flight performance and mission capability. Realization of such versatile flapping mechanism with additional ability of producing thrust levels that fulfill requirements of cruising forward flight and vertical take-off and landing (VTOL) conditions demand extensive design validation and performance evaluation. This paper presents a concerted approach for mechanism development of a 20 cm span flapping MAV through an iterative design process and synergistic fabrication options involving electrical-discharge-wire-cutting (EDWC) and injection molding. Dynamic characterization of each mechanism is done through high speed photography, power take-off measurement, wind tunnel testing and proof-of-concept test flights. The research outcome represents best-in-class mechanism for a 20 cm span flapping MAV with desirable performance features of extra-large flapping stroke up to 100°, minimal transverse vibrations and almost no phase lag between the wings.

1. INTRODUCTION

1.1 General description of flapping micro air vehicles

Among the many variants of micro air vehicles, the flapping vehicle has garnered substantial interest and attention for the past few years due to its superior maneuverability and associated applications that include surveillance, reconnaissance, search and rescue missions. A survey of the substantial published literature on the aerodynamics of flapping wings [1-5], unsteady state models [2, 6], quasi steady state models [7], fluid-structure interaction [8-11] and aero-elasticity [12-13] indicates that, the data pertaining to design and fabrication of light-weight and efficient flapping mechanisms is limited. While the mechanisms of biplane flapping MAVs witnessed a few development efforts, the monoplane mechanisms that are capable of vertical take-off and landing (VTOL) have largely remained unexplored options for many years. Published literature [14-17] indicates the demonstration of VTOL ability and large payload capacity by biplane MAVs owing to their wing area that is almost 200% that of a monoplane. The development of a monoplane flapping mechanism capable of VTOL needs a high degree of understanding on the nature's flapping principle and mechanism [18-20]. Also, a greater amount of work goes into refining the mechanism to draw optimized power from the battery and sustain flight for a prolonged time. In many cases, a four bar linkage (FBL) mechanism shown in Fig. 1 is selected for this purpose because of its simplicity and versatility [2-4, 7, 10-11, 21-22]. As can be readily inferred from the reported studies, the phase lag between two wings is inevitable and large flapping strokes indicate high phase lag.

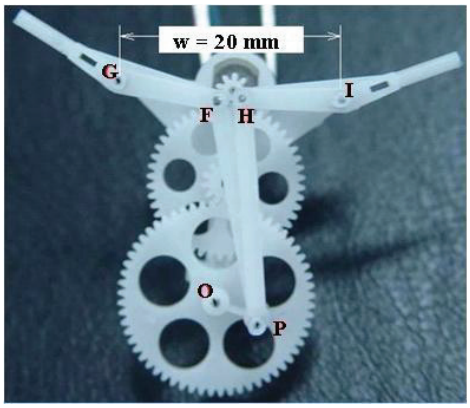

Figure 1. FBL mechanism used in the flapping MAV "Golden Snitch" [22]

1.2 Survey on the phase lag and the flap angle of flapping mechanisms

In the previous work [4] of the authors, polyvinylidene fluoride (PVDF) sensor was used to measure the in-situ lift force of a flapping MAV. It distinguished the phase lag of lift force which is caused due to the inherent nature of FBL mechanism. Figure 2 reveals that, the phase lag due to lift force experiences increase in trend at around 6.5° of mechanical or the gear-transmission lag. Such tendencies may influence the deterioration of lateral stability of the flapping MAVs. However, the birds in real world with 120° flap angle have positive effect on the aerodynamic characteristics [23]. Therefore, authors examined earlier development efforts of flapping mechanisms [24-58] and inference on their kinematic performance with respect to the phase lag and flap angle which are given in Table 1.

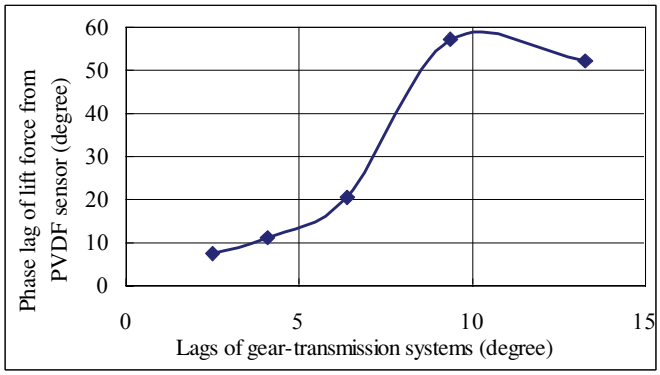

Figure 2. Deduced phase lag of lift force from the PVDF sensor measurement

The authors categorized the previous works on the development of flapping mechanism based upon the crank rocker mechanism [24-27], FBL mechanism [4,10-11, 21-22, 28-34], other kinematic structural FBL [35-40], slider crank mechanism [41-42], 6 links mechanism [43-45], combination of various mechanism to achieve the desired motion characteristics [46–53], rigid body model of wing motion [54–57] and also a mathematical model of flapping wing as a beam [58]. It is evident from the Table 1 that, the information pertaining to the phase lag and flapping angle is not documented clearly in majority of the studies. In most of the instances, phase lag causes deterioration in the performance with reference to the VTOL and hovering.

Hsu *et al*. [59] proposed 12 flapping mechanisms based on the topological structure and their motion characteristics. These mechanisms have one degree of freedom which simulates wing motion of long ear bats and insects and no studies have been carried out for the flapping motion characteristics such as phase lag and flapping angle. Ryan [60] classified ten planar, two spherical and three spatial mechanisms based upon the workspace, topology, actuator type and transmission mobility. A comprehensive survey [61] of various flapping wing vehicles and their mechanisms such as Delfly I and II from Delft University, Wing differential I and II from Berkley, VTOL MAV from DRDO, India,

Table 1. The phase lags and the flap angles for different flapping mechanisms

Previous work	Phase lag (degree)	Flapping angle (degree)	Remarks
Fenelon *et al.*, [24], 2010	NI	90°	Crank-link mechanism
Fujikawa *et al.*, [25], 2007	NI	150°	Butter fly type crank-link mechanism
Ge *et al.*, [26], 2013	0°	76°	Crank-link mechanism
Wang *et al.*, [27], 2010	1°	+/- 24°	Single-crank with double-rocker mechanism
Yang *et al.*, [4], 2007	5°	61°	FBL
Yang *et al.*, [10-11, 21-22] 2009-2012	3°	53°	FBL
Khatait *et al.*, [28], 2006	3°	40°	FBL
Yan *et al.*, [29], 2001	20°	+/- 70°	FBL
Tanaka *et al.*, [30], 2005	NI	74°	FBL
Isaac *et al.*, [31], 2006	180°	160°	FBL
Syaifuddin *et al.*, [32], 2006	NI	80°	FBL
Finio *et al.*, [33], 2009	0°	±60°	FBL
Hubel *et al.*, [34], 2009	NI	44°	FBL
Wood [35], 2007	NI	NI	3 DOF FBL
Lai *et al.*, [36], 2005	NI	+/- 50°	FBL with belt drives
McDonald *et al.* [37], 2010	NI	68°	Spherical FBL
Park *et al.*, [38], 2012	0°	42°	2 FBL
Han *et al.*, [39], 2010	20°	120°	A pair of FBL
Teoh *et al.* [40], 2013	30°	50°	2 FBL
Madangopal *et al.*, [41], 2006	NI	+/- 90°	Slide crank - link mechanism with springs
DiLeo *et al.*, [42], 2007	5°	+/- 50°	Slider crank mechanism
Khan *et al.*, [43], 2007	NI	±90°	6 link mechanism
Mukherjee *et al.* [44], 2004	NI	NI	6-link mechanism
Lentink *et al.*, [45], 2008	90°	NI	Pantograph mechanism
Banala *et al.*, [46], 2005	7.9°	90°	Combination of 5-bar and FBL mechanism
Avadhanula *et al.*, [47], 2003	20°	120°	Combination of 2FBL mechanism and spherical wing differential mechanism
Zbikowski *et al.*, [48],2005	NI	+/- 45°	1. FBL figure-8 generator 2. 2 wing articulations 3. Geneva wheel for rapid pitch reversal
Yokoyama *et al.* [49], 2008	NI	NI	Combination of 3-link mechanism and pantograph mechanism
Park *et al.* [50-52], 2014	0°	92°	FBL+slider crank
Keennon *et al.* [53], 2012	NI	>120°	2-FBL in series
Yan *et al.*, [54], 2003	NI	80°	2 DOF rigid body wing
Maybury *et al.*, [55], 2004	NI	120°	3D robotic dragonfly mechanism
Thomson *et al.*, [56], 2009	NI	45°	3DOF rigid body model
George *et al.* [57], 2012	NI	NI	3 DOF differential driven mechanism
Mukherjee *et al.* [58], 2010	NI	+/- 35°	Flapping structure is considered as beam

- NI No Information
- FBL – Four Bar Linkage

small and Jumbo bird from University of Maryland, HMF and PARIT Y from Harvard University, Lissajous MAV from Cranfield University are presented to delineate the salient features. Gerdes [61] categorized the flapping mechanisms into double push rod, double crank, single pushrod, and side mounted crank and compared each of them based upon flapping motion and design performance.

Recently the MAV work in Konkuk University combined the FBL and slider mechanism achieving flap angle beyond 90° and 17 Hz frequency with almost zero phase lag [50-52]. Their small sliding stroke design improved the friction issue of Refs. [41-42] and is good for the VTOL.

A greater amount of work goes into refining the mechanism to draw optimized power from the battery and sustain flight for a prolonged endurance. The major problem faced with the monoplane flapping mechanism besides lack of sufficient forces for VTOL is the phase lag between the left and right wings during flapping. Phase lag of less than 3° results in an intrinsic level-turning behavior for the flapping MAV in its trajectory and less asymmetric lifts for both the wings [4, 10-11, 21-22]. A conventional approach is taken in the design of such mechanisms where the number of linkages is kept at minimum, to reduce the overall weight of the gearbox and to mitigate the loss in the performance due to friction in linkage vertices. While this has a great benefit in terms of the light weight and high efficiency, nevertheless, it is not suitable for production of higher wing beat amplitudes or the flapping stroke. In most cases, the beat amplitude is limited to flap angles far less than 90° except the "Nano Humming bird" developed by AeroVironment Inc. [53]. It is known that, by adjusting the linkage lengths of FBL of Fig. 1, it is hard to achieve maximum or minimum flap angle and phase lag at the same time. Hence, the design goal of large flap angle and small phase lag could be realized by the ingenious design of "Nano Humming bird" in-spite of its dependence on a very powerful electric motor for generating driving torque.

The choice of the mitigating mechanism is an elaborate process, as it constrains the amplitude of the wing beat, while helping to reduce the phase lag. It is also essential to maximize the flapping angle with almost zero phase lag to achieve maximum lift from a single cycle. Hence, this paper presents the improvement of the authors previous FBL mechanism of "Golden Snitch" [10-11, 21-22] with an addition of Watt and Evans straight line mechanisms [62-66] to obtain zero phase lag, to avoid the overturning of the vehicle and also to accomplish higher flapping angle for the enhancement of lift force during a wing beat cycle. Evans and Stephenson (Watt) mechanisms are the category of non-grashof double-rockers that can generate an approximate straight-line motion. In comparison with the well-known Watt mechanism, Evans mechanism could provide a more compact design for the present development of MAV of 20 cm wingspan. The designed mechanisms were fabricated using EDWC and the plastic injection molding, and validation is performed through wind tunnel and flight test experiments.

2. FLAPPING MECHANISM DESIGNS

2.1 Conventional FBL

Early attempts of the authors in the year 2007 led to the development of a kinematic model with a FBL mechanism (Fig. 1) for a 20 cm wingspan flapping MAV called "Golden Snitch" [10-11, 21-22]. It was driven by a 6mm motor with a gear reduction of 26.67 and test flights with an endurance of 480 seconds. This mechanism featured two branches (OPFG and OPHI) and the hinge points F and H were not coincident leading to a phase lag between two wings. The marked hinge positions shown in the Fig. 1 as OPEG and OPHI can be changed and several iterations will be carried out to achieve an effective linkage dimension. As they were unable to move along a vertical trajectory, vertical takeoff could not be accomplished. Further, simulation using a free computation code Flap design 2.2 JAVA [62] revealed a flapping angle of 53° with a phase difference of 3° (Fig. 3 [4, 22]) could be achieved through this mechanism. In the simulation, flapping angle is restricted due to the linkages dimension and hinge positions to avoid singularity position where the mechanism ceases in their fully extended and contracted

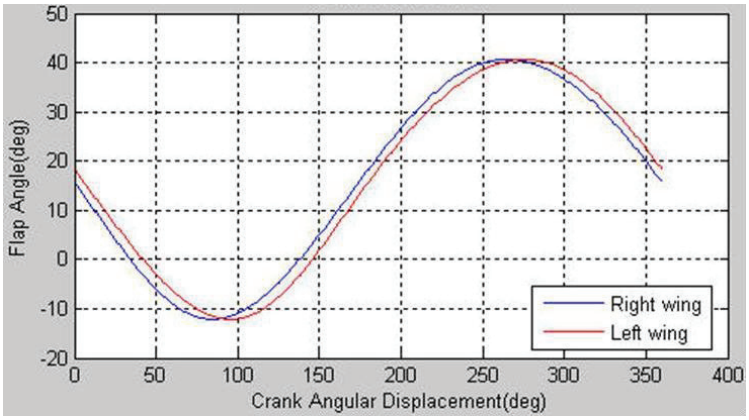

Figure 3. Flap angle with phase lag of conventional FBL [4, 22]

positions. In addition, during the large flapping strokes, the phase lag is reached to a maximum of 3° between right and left wings. As the flapping of both the wings depended solely on the crank and follower guided by a gear train, the phase lag could induce a right-ward turning moment deterring the turning performance on the left side and consequential reduction in the life cycle of the mechanism.

2.2 FBL with Watt mechanism-Stephenson mechanism

In order to overcome the above referred phase lag, inclusion of Watt mechanism [63] into conventional FBL is proposed as represented in Fig.4 (a). By introduction of Watt mechanism (BCADE), the authors are able to create figure-8 trajectory and also the central linkage is able to execute straight line motion enabling the propelling of flapping MAV in the vertical direction. The combination of FBL and Watt is named as 3rd type of Stephenson six- link mechanism (simplified as Stephenson mechanism, in further sections) [64-65]. Table 2 shows the dimensional details of various linkages of the Stephenson mechanism that are proposed to propel a 20 cm wingspan flapping MAV with a vertical take-off. The Watts mechanism ensure the straight line motion of a point A by ensuring the ratio of lengths of links of CA to AD is equal to the ratio between DE and BC.

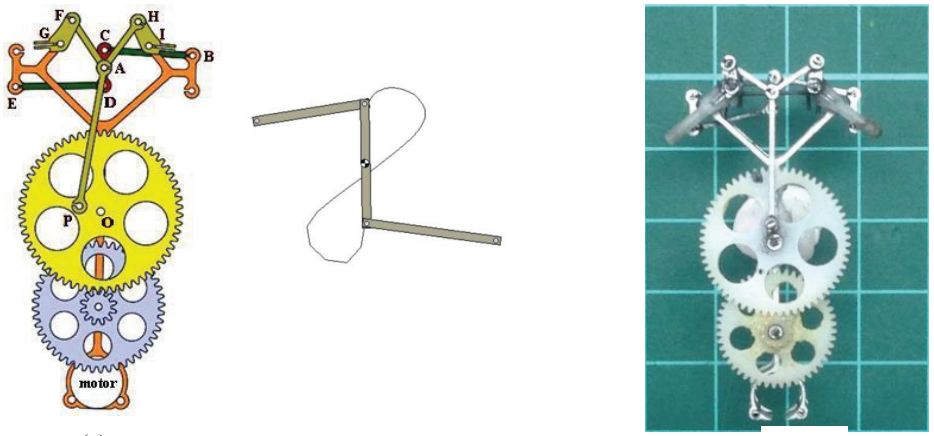

Figure 4. (a) Integration of Watt mechanism with FBL (b) The figure-8 trajectory of Watt mechanism [63] and (c) Prototype of Stephenson mechanism

To ensure light weight mechanism with adequate structural integrity, authors used EDWC technique to manufacture the mechanism linkages with Al-alloy 7075 and assembled them together with an aid of tiny stainless steel needles. The mechanism has a gear reduction ratio of 26.7 and the prototype with injection-molded gears is developed for experimental trials. Studies to evaluate the kinematic performance of Stephenson mechanism assure that, the mechanism can attain a flapping angle of 70° with zero phase lag (Fig. 5.) A practical study of the mechanism unveil operational challenges such as

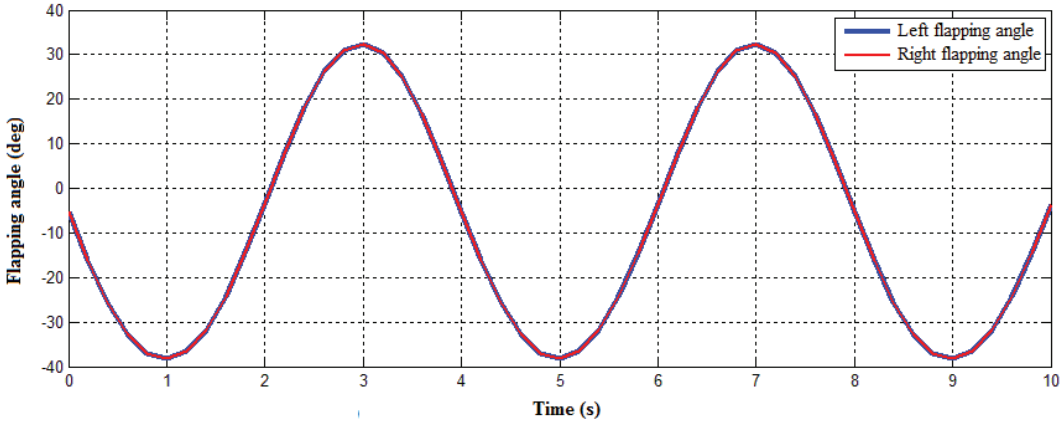

Figure 5. Flapping angle of left and right wings of Stephenson mechanism

Table 2 Dimension of the Stephenson mechanism

Component	Size (mm)
Base width (BE)	20
Base height (OA)	19
Linkage width	0.7
1st bar (OP)	2
2nd bar (PA)	16
Control bar (CD=2CA)	4
Side bar (DE=BC)	10
3rd bar (AF)	6.5
Wing bar (FG)	3 (120°)
Max flap stroke angle	70°

high vibration levels, susceptibility of lengthy linkages (BC and DE) to bending and challenges in placement of motor without affecting the flight stability.

Real time capturing of flapping motion of the Stephenson mechanism is carried out using a high-speed CCD camera (Phantom V 4.2) with the driven voltage of 3.7V. The wing beat cycle of the Stephenson mechanism for the up and down stroke angle during the continuous motion is captured which is shown in Figs. 6 (a) - (h). It can be observed from the experimental results in Fig.7 (a) that,

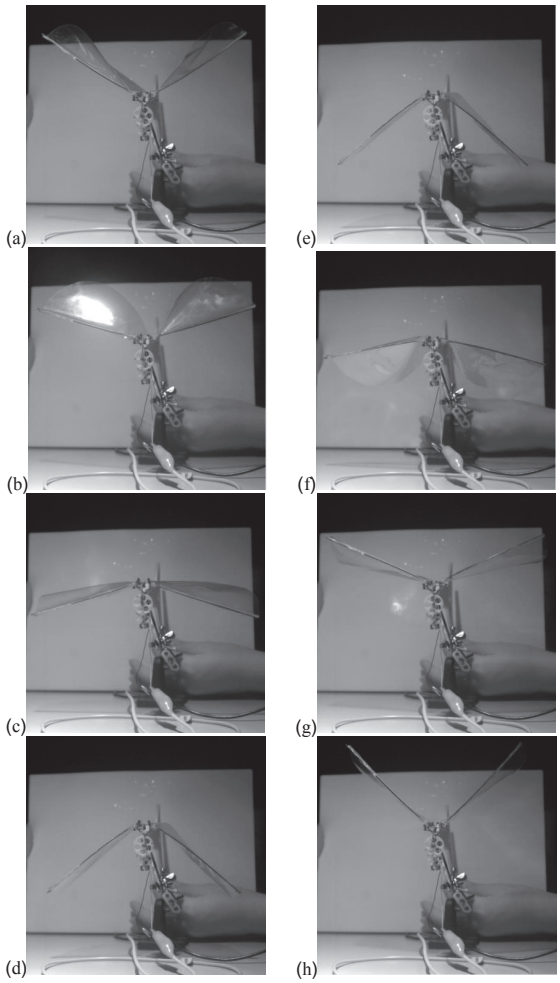

Figure 6. Wing beat cycle of Stephenson mechanism

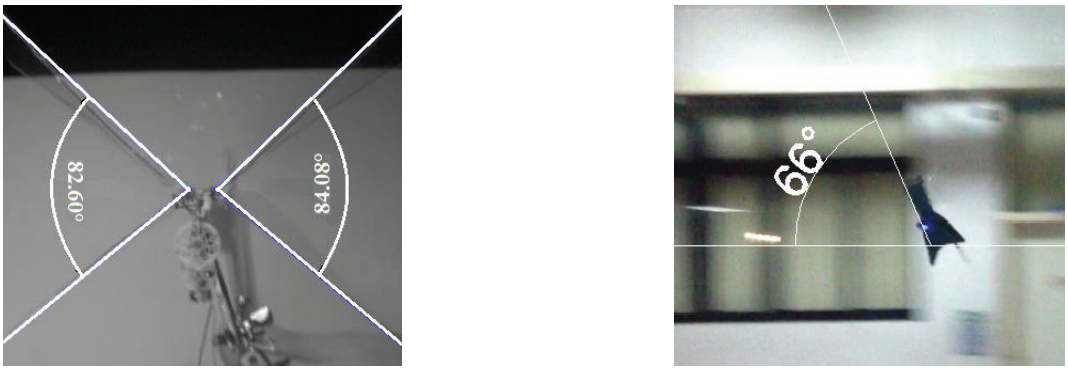

(a) (b)

Figure 7. FBL with Stephenson mechanism: (a) Measurement of flapping angle using a high-speed camera; (b) Flight test of the MAV Golden Snitch using Stephenson mechanism and the instantaneous AOA is 66°.

the Stephenson mechanism is able to demonstrate good flapping characteristics with a maximum flapping angle of 84.08° on the right wing with a phase lag of 1.48°. The flapping frequency of 14Hz with an instantaneous angle of attack (AOA) of 66° is attained during the flight test as shown in Fig. 7(b).The stable flight has accomplished maximum flight endurance of about 57 seconds to reach an altitude of 2m.

FBL with Evans mechanism

Despite the fact that the aforementioned Stephenson mechanism is able to reduce the phase lag to minimal level, it induces high vibrations during flapping and necessitates considerably high space in the lateral direction of the structure. To ensure the compactness of the flapping mechanism and also to achieve the straight line motion, Evans mechanism is considered for further studies. The proposed mechanism would reduce the number of linkages compared to the Stephenson mechanism that leads to reduction of overall weight of the mechanism structure and also the flapping motion characteristics can be enhanced. In earlier time, Evan mechanism [66] was used in cranes to move the containers along a prescribed axis in a straight line so as to make sure the smooth linear motion. Due to the facts such as, structural simplicity of mechanism, minimum number of linkages than Stephenson mechanism (9 links in Stephenson mechanism and 8 links in Evans mechanism), and less weight necessitates the Evans mechanism in the design of MAVs. The placement of motor at the top of the mechanism (motor is placed at the bottom in Stephenson mechanism) will result in the reduction of centrifugal effect and consequent moment that makes the system to relieve the stresses and strains on the body structure compared to the Stephenson mechanism. In addition, Evans mechanism occupies less space than the Stephenson mechanism that suits for the development of Ornithopter mechanism [67] structure. The performance evaluation of FBL with Evans mechanism is carried out by designing and assembling mechanism linkages as shown in Fig. 8 (a) where a point A will move along the vertical straight line to ensure the VTOL of the vehicle and Fig. 8 (b) shows the exploded view of the mechanism assembly.

The flapping characteristic of FBL with Evans mechanism is studied through kinematic simulation using Autodesk Inventor. Evans mechanism created flapping angle of 80° (Fig. 9) with zero phase lag which is higher than Stephenson mechanism and the compact design of the structure ensures the stability of vehicle without much vibration. The complete linkage dimensions considered for the design pertaining to FBL with Evans straight line mechanism is shown in Table 3.

In addition, the straight line motion of a point A is ensured by maintaining the ratio of links between DE and CD equal to the ratio between CD and AD.

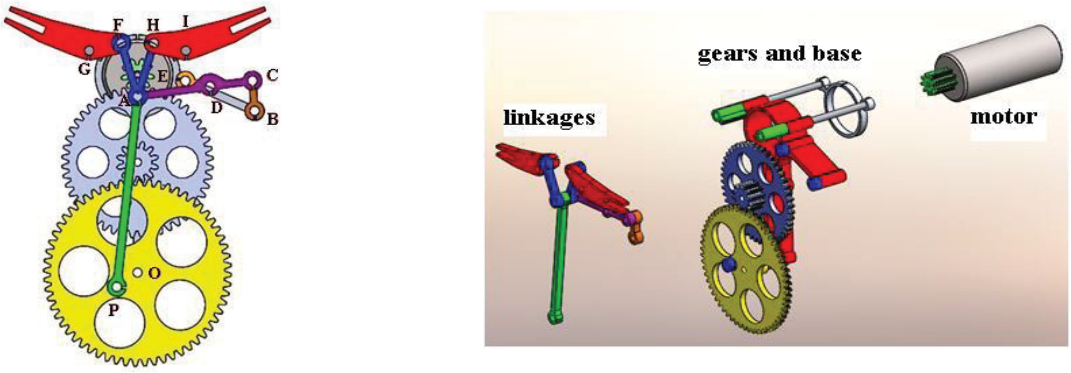

(a) (b)

Figure 8. (a) FBL with Evans straight line mechanism assembly; (b) Exploded view of mechanism

Table 3 Dimension of the flapping mechanism with Evans straight line mechanism

Component	Size (mm)
1st bar (OP)	2.5
2nd bar (PA)	19
3rd bar (AF)	5.516
Wing bar (FG)	3.25
Control short bar(DE)	2.5
Control medium bar(CB)	3
Control long bar(AC=AD+CD)	11.475=7.225+4.25

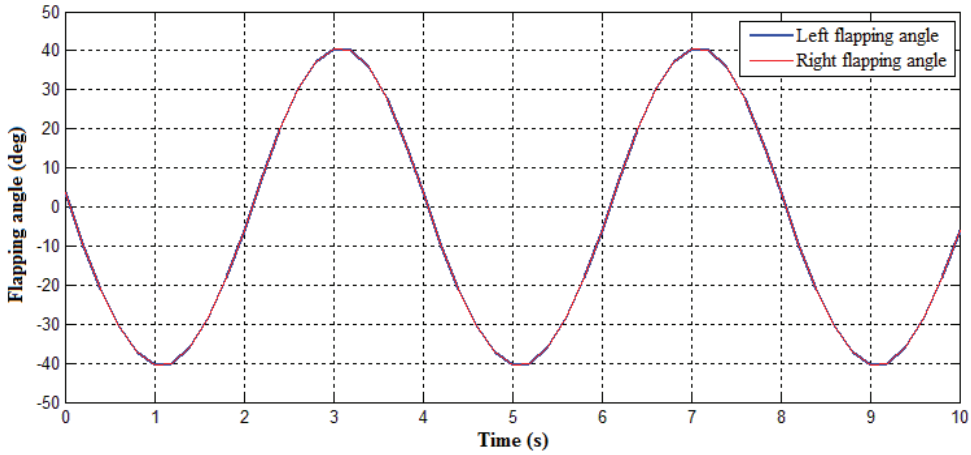

Figure 9. Flapping angle of left and right wing of FBL with Evans mechanism

In order to examine the flapping characteristics, CCD motion capture system, captures the wing beat cycle of the Evans mechanism as given in Figs. 10 (a) - (h) that clearly indicates up and down stroke angle of the developed mechanism. The experimental investigations on the Evans mechanism confirms the maximum flapping angle of 100.43° [Fig.11 (a)] and AOA of 77.94° [Fig.11 (b)] is achieved in the real time flight tests which is higher than the Evans mechanism test flight results shown in Fig. 7 (a)

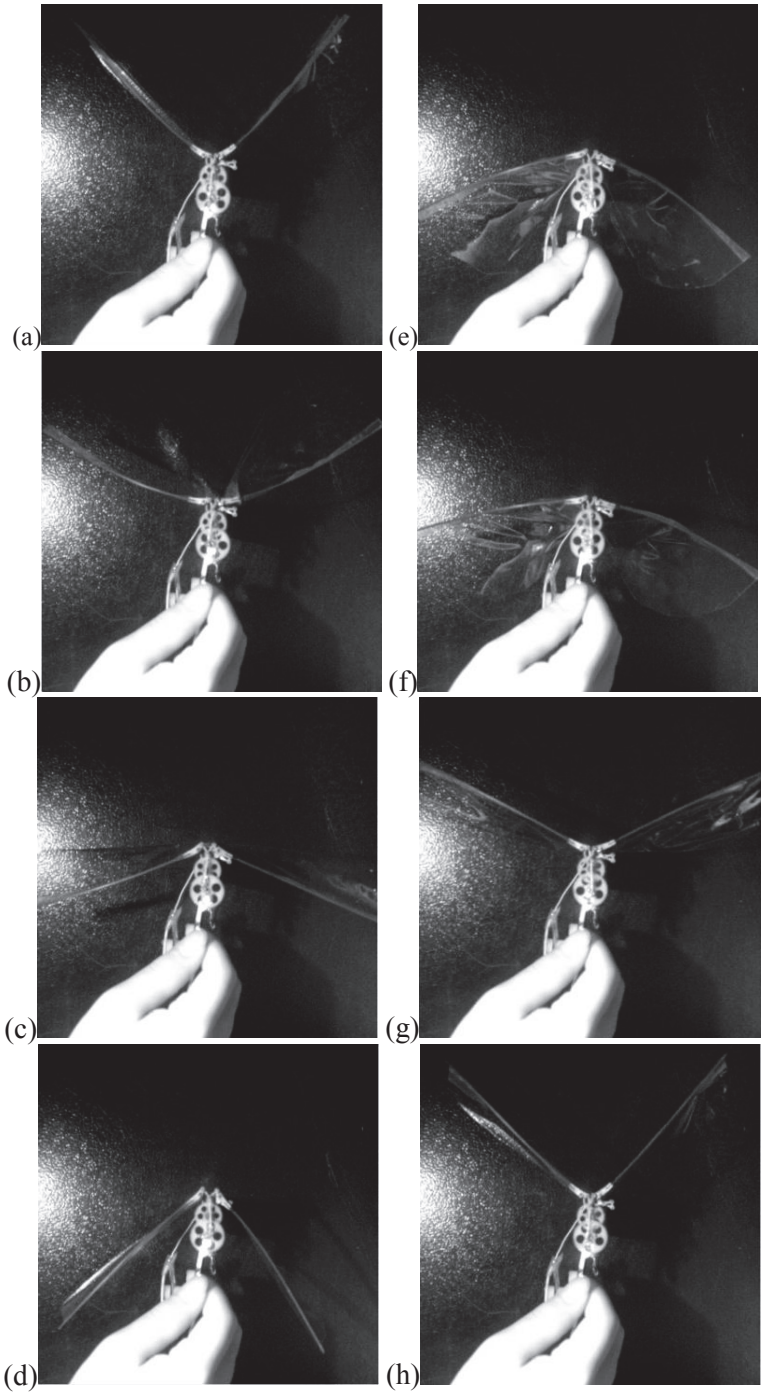

Figure 10. Wing beat cycle of Evans mechanism

and (b). Also, the flapping frequency is increased to 18 Hz; flight endurance is improved to 120 s and the developed vehicle reach altitude of 20m in 20s. More video demonstration of the test flight could be referred to YouTube website of https://www.youtube.com/watch?v=fbQV0nZqS6o. These results affirm that FBL with Evans mechanism has better aerodynamic performance characteristics than Stephenson mechanism.

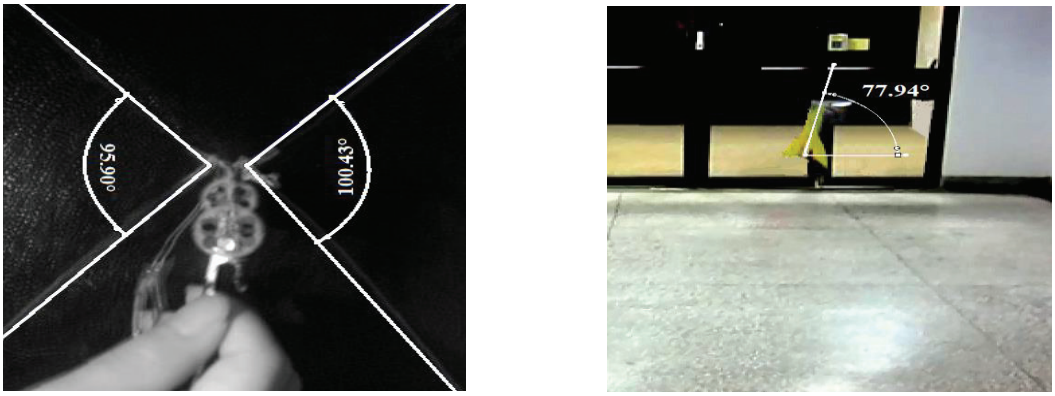

(a) (b)

Figure 11. FBL with Evans mechanism: (a) Measurement of flapping angle using a high-speed camera; (b) Flight test of the MAV Golden Snitch using Evans mechanism and the instantaneous AOA of 78°.

It can found that the total flap angle in Figs. 7 and 11 appears larger than the predicted ones in Figs. 5 and 9. The reason is due to the high flexibility of the flapping wing, especially the carbon fiber wing-spar at the leading edge. The Solidworks simulation of Figs. 5 and 9 is based on the rigid assumption of mechanisms. Rigidity of the gear transmission is still high with no increase in flap angle. The rigidity of the gear transmission has not influenced the flap angle in theoretical as well as real time testing. However, at the moment of the stroke reversal during a high-frequency flapping the stroke angle exceeds the limit that SolidWorks predicts in Figs. 5 and 9. In other words, the obvious bending of the carbon fiber wing-spar contributes the apparent increase of flap angles of 12-14° in Fig.7 (70°→82-84°) and 16-20° in Fig.11 (80°→96-100°) during the vigorous wing flapping.

In addition, the performance evaluation of these mechanisms is summarized and given in Table 4. It is observed that, the Evans mechanism has better flight endurance, pay load capacity and low power consumption for the same capacity of the battery.

Table 4 Mechanism performance comparison

Mechanism	Battery and its specification	Flight endurance (s)	Power consumption (W)	Empty weight (g)	Payload (g)
FBL with Stephenson mechanism	60mAH, 3.7 V max.	57 s	14.02 W	10.46 g (2.44g mechanism)	0.54 g
FBL with Evans mechanism	60mAH, 3.7 V max.	120 s	6.66 W	9.62 g (1.48g mechanism)	1.38 g
● Flight endurance (s) = 0.060 AH (battery charge)* (3600 s/H)/ (Power consumption/ 3.7 V) ● Payload= 11g (body mass predicted by the scaling law [23]) - Empty weight					

3. FABRICATION AND ASSEMBLY OF FLAPPING MECHANISM

The authors have preferred the plastic injection molding (PIM) [22] as the option for the fabrication of mounting bracket, linkages and gears due to inherent advantages such as wide range of material options, availability of fillers for strength enhancement, low wastage and cost-effective transformation to mass production. The material chosen for the fabrication trials is polyoxymethylene (POM) due to its toughness, low coefficient of friction and excellent dimensional stability. The mounting bracket shown in Fig. 12 is designed and fabricated to accommodate various sizes of gears at different positions to achieve gear reduction ratios of 16, 20, 21.3, and 26.67 respectively.

In addition, Evans mechanism linkage components designed by SolidWorks software are shown in Fig. 13.

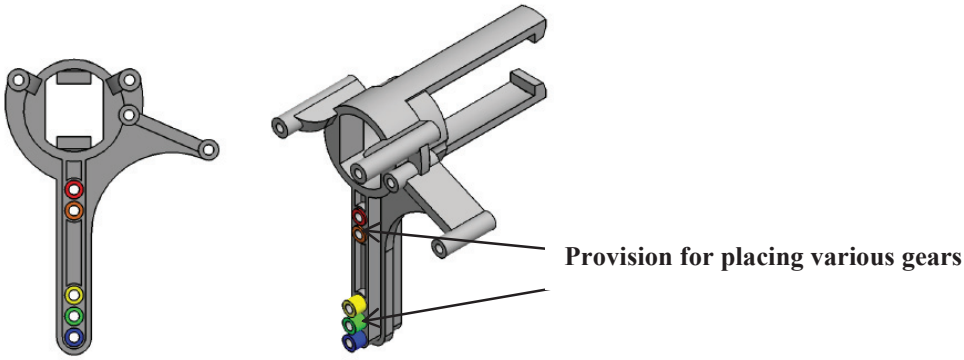

Figure 12. Gears and motor mounting frame manufactured using PIM

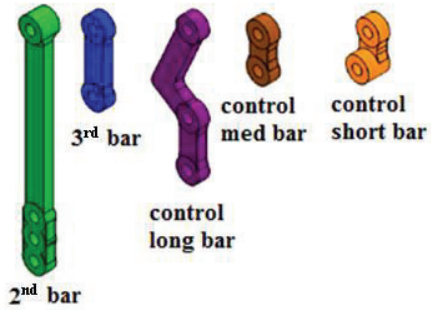

Figure 13. CAD model of Evans mechanism components

Wing spar FG and HI are designed in such a way that, they can accommodate the carbon fiber spar into this wing bar housing as shown in Fig. 14 at the leading edge of the wing. When the carbon fiber spar is firmly inserted into the housing without allowing any rotation, the developed flapping MAV will have a forward flight as shown in Fig. 15. However, the hovering flight can be accomplished when the carbon fiber rod rotates freely in the wing bar housing (Fig. 16.) These design features ensure an efficient control on the inclination of wing plane and wing assembly including attainment of Figure-8 motion.

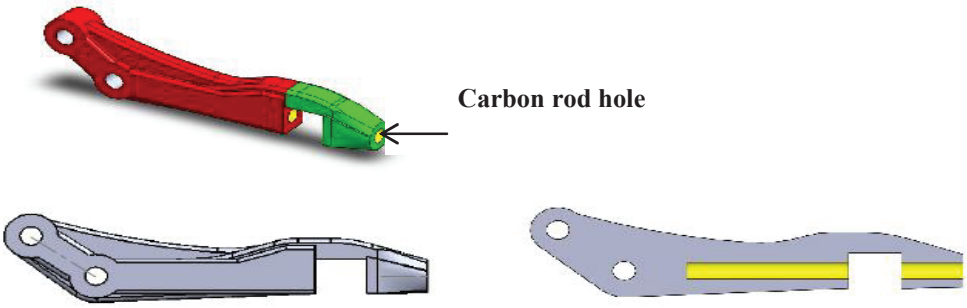

Figure 14. Wing bar and its housing design

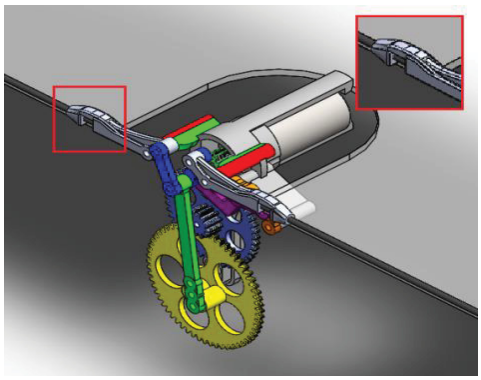

Figure 15. Wing assembly for forward flight

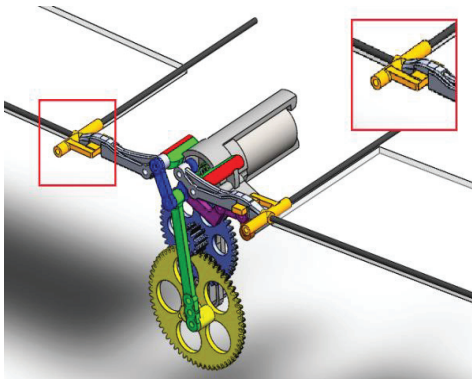

Figure 16. Wing assembly for hovering

Figures 17 and 18 show the injection mold and the resultant injections of the mechanism components respectively. Total weight of the mechanism assembly realized through injection molding is 1.48g which is 39% of lighter than EDWC fabricated mechanism (Fig. 19). Table 5 compares the performance characteristics of Evans mechanism which are made up of Al-alloy through EDWC and POM with PIM process, where in the former achieved superior characteristics than later.

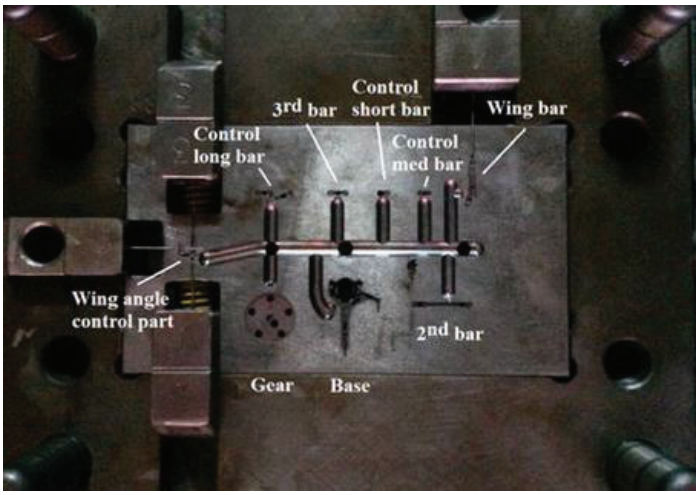

Figure 17. Plastic injection mold for producing Evans mechanism linkages

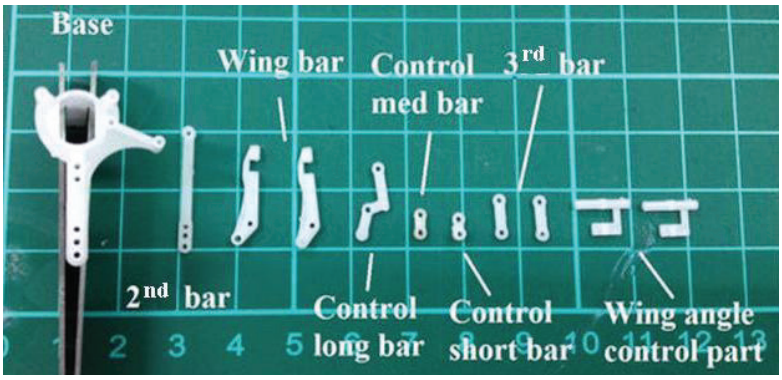

Figure 18. Plastic injection molded parts of Evans mechanism linkages

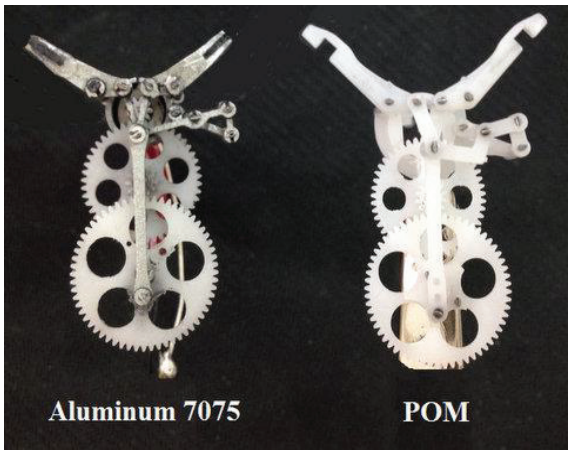

Figure 19. FBL with Evans mechanism assembly, using Al-alloy7075 by EDWC, and POM by PIM; All the gears are made by PIM.

Table 5 Comparison of two Evans mechanisms; 20 cm wing, 3.7 V driving

	Al-alloy 7075 by EDWC	POM by PIM
Weight (g)	2.44	1.48
Phase lag (design value=0°)	4.53°	2.05°
Max. flapping angle (design value=80°)	100.43°	83.1°
Flapping frequency (Hz)	18.86	13.51

The comparison is also made in the time taken aspects of fabrication, mechanical linkage assembly, and also other parts including gear assembly which are given in Table 6. The plastic injection molded part is manufactured and assembled in 21 min which is far lesser than EDWC technique.

Table 6 Time taken for manufacturing and assembly of Ornithopter mechanisms

Different ways of fabrication/ assembly	Mechanism manufacturing (min)	Mechanical assembly (min)	Other parts assembly (min)	Total fabrication/ assembly time(min)
FBL with Stephenson mechanism by EDWC	50	35	10	95
FBL with Evans mechanism by EDWC	45	30	10	85
FBL with Evans mechanism by POM injection molding	1	10	10	21

4. RESULTS AND DISCUSSION

4.1 Motor torque requirement: without wings

In order to ensure the motor torque requirement for the various gear reduction ratio, experimental analysis has been carried out.

$$T = \frac{P}{\omega} = \frac{IV}{\omega} \tag{1}$$

Equation (1) relates the input current (I), voltage (V), angular velocity of the driver (ω) to the torque (T).

With an assumption of negligible motor loss and also 100 % motor efficiency, the experiments are conducted to measure the flapping frequency and torque without the usage of tachometer and torque meter. During the course of experiments, by varying the voltage, the corresponding motor current is measured which directly provided the power requirement of the mechanisms. In addition, flapping frequency or rotation speed of the motor is determined through the high speed camera motion capture system. These measurements were plotted for various gear ratios of mechanism to evaluate the performance of the developed mechanisms.

The requirement of torque for the various gear ratios of Evans mechanism without wings (manufactured using Al-alloy 7075 in EDWC) such as 16, 20, 21.3 and 26.67 are experimented through varying the flapping frequencies. The results suggested that for the achieved maximum flapping frequency of 19 Hz, the Evans mechanism with gear ratio of 26.67 is suitable because of lowest torque to work as shown in Fig. 20. The other gear ratios of Evans mechanism may increase the size of the motor and simultaneously increase the overall weight of the system.

In addition, experiments were conducted to obtain the torque characteristics on Stephenson and Evans mechanism for the gear reduction ratios of 21.3 and 26.67. The result shown in Fig. 21 has proved that, torque requirement is higher in the Evans mechanism with gear ratio of 21.3 than 26.67 and remains constant in most of the cases. However, in the Evans case of gear reduction 26.67, the torque and load carrying capacity increase linearly with flapping frequency as shown in Figs. 20 and 21. It denotes the load-free operation of Evans gear ratio 26.67 is frequency-dependent and may be caused by the tighter assembly of this mechanism. However, this required torque of the flapping

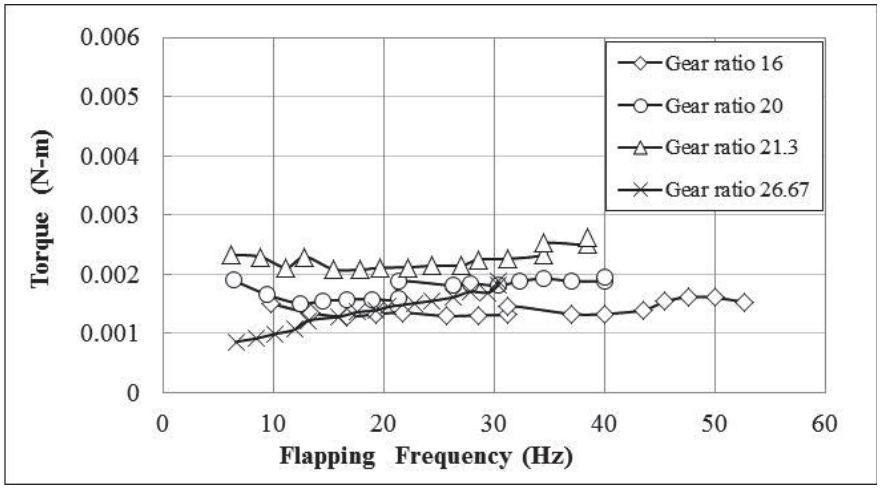

Figure 20. Effect of gear ratio of Evans mechanism on the torque requirement

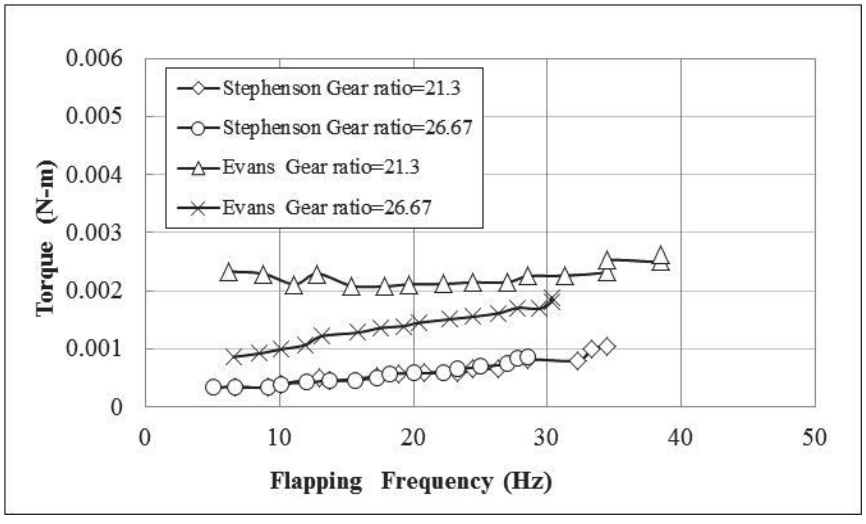

Figure 21. Comparison on the torque requirement of Stephenson and Evans mechanism

mechanism will be showed at least one-order of magnitude smaller than the total required torque in the next section, and can be regarded as a minor factor in this study.

In the event of gear ratio 21.3 and at the flapping frequencies 34.48Hz and 38.6 Hz, there were overlapping behavior occurs in the flapping frequencies due to the frictional obstruction in the mechanism. This can be overlooked with an increase in power through avoiding the particular flapping frequency.

4.2 Motor torque requirement: with wings

The similar sets of experiments were performed on Evans mechanism attached with wings of 20 cm span with a semi-elliptical wing area of 123.4cm^2 [10-11, 21-22]. The wing design for both the two flapping mechanisms is shown in Fig. 22. "Golden Snitch" has a flexible wing frames. The wing is composed of carbon-fiber leading-edge spar (of 0.8 mm in diameter) and polyethyleneterephthalate (PET) wing skin (of 24 mm thick). The detailed description about the mechanical stiffness can be referred in [11, 21] where the effect of wind speed is completely described.

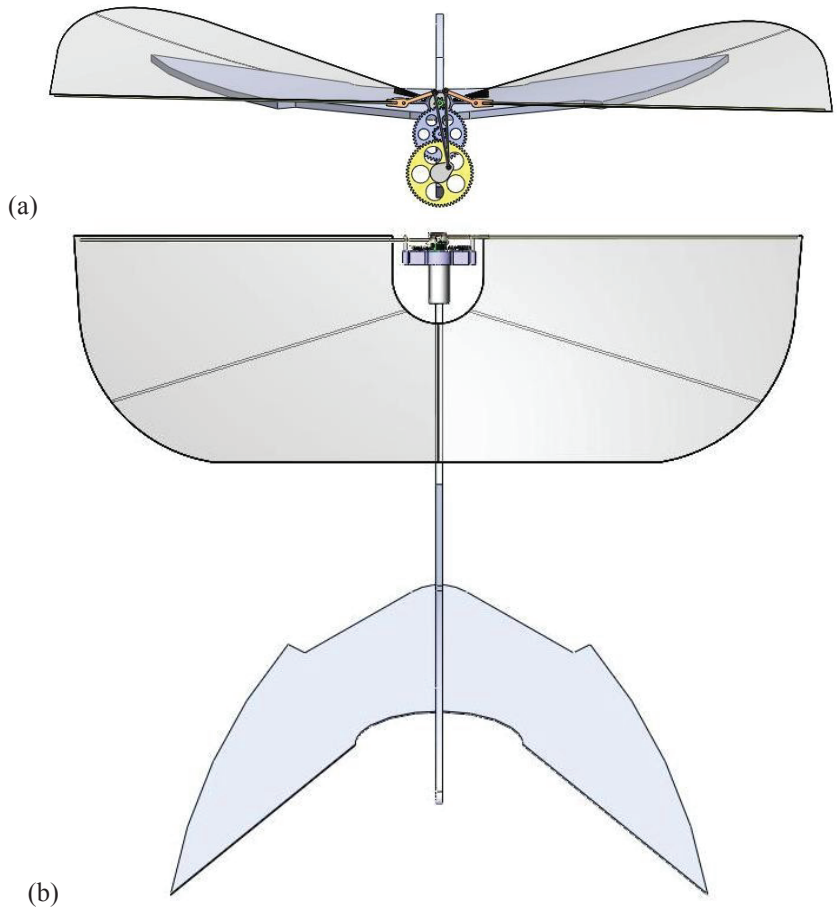

Figure 22. The "Golden Snitch" MAV with wing area of 123.4 cm^2: (a) front view; (b) top view

Through varying the gear reduction ratios, the torque requirements are assessed in Fig. 23. In all these cases, the torque requirement is found to increase with the flapping frequency almost linearly. For the gear ratio of 26.67 with the flapping frequency approaching 19Hz, the torque required is the least among all the configurations.

Also, Figure 24 endorses that, both Stephenson and Evans flapping mechanisms with higher gear reduction ratio necessitate a small motor with less torque to achieve high flapping frequency. Between these two mechanisms, larger torque is required for the Stephenson mechanism than that of the Evans mechanism due to higher friction and larger power loss.

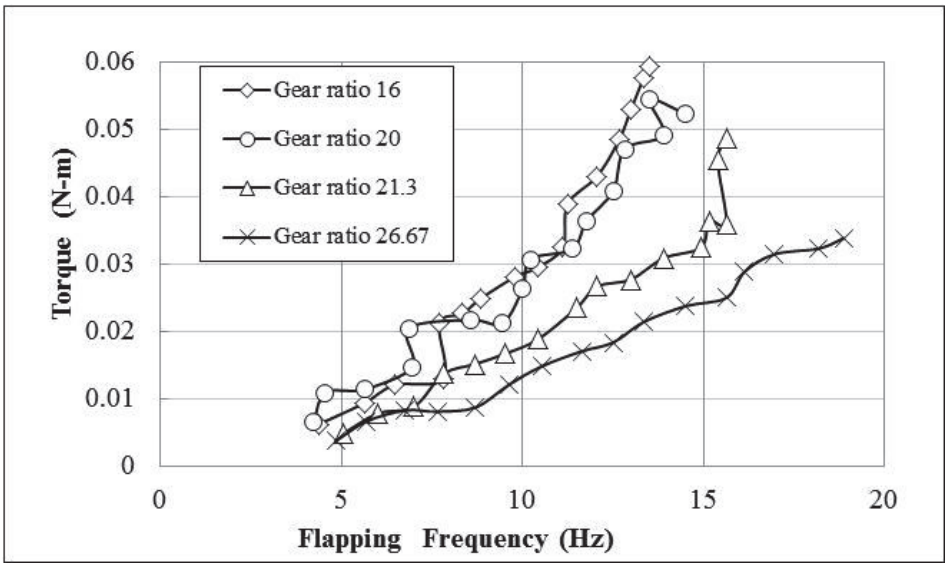

Figure 23. Effect of gear ratio of Evans mechanism on the torque requirement

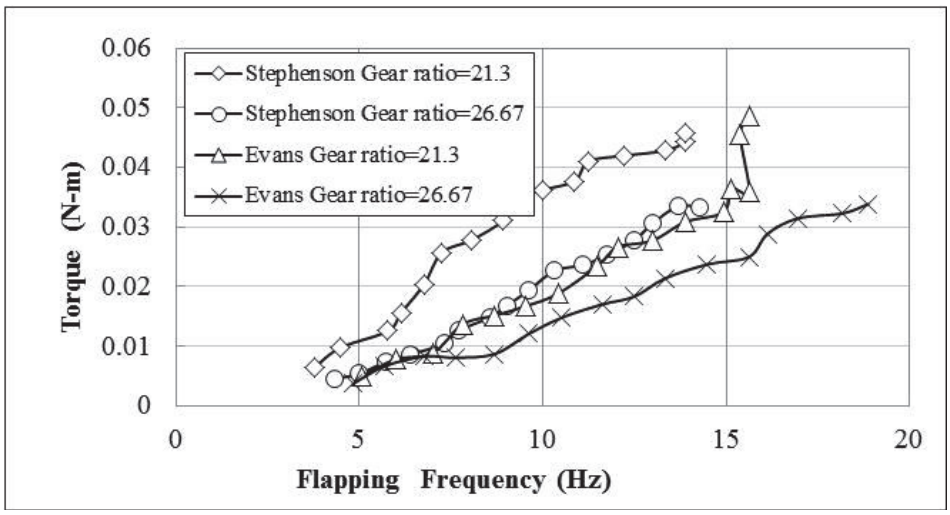

Figure 24. Effect of gear ratio on torque requirements of Stephenson and Evans mechanism

The aerodynamic performance characteristics of Stephenson and Evans mechanism are compared and provided in Table 7 in which, frictional effect is predominant in the case of Stephenson mechanism in comparison with the Evans mechanism. These measurements were carried for the identical wing planform of both the mechanisms.

Table 7 Overall performance comparison of mechanisms

Measurement at 3.7 V driving voltage	Stephenson mechanism	Evans mechanism
Flapping angle	82-84°	96-100°
Flapping frequency	14.3 Hz	18.9 Hz
Total Power consumption	14.02 W	6.66 W

4.3 Wind tunnel testing

For aerodynamic characterization of these developed mechanisms, wind tunnel testing is carried out at various angles of attack (AOA) in the range of 20°-70°. The test section has dimensions of $30 \times 30 \times 100$ cm^3 and the inlet contraction ratio is 6.25. The wind tunnel with the flapping MAV placed on the load cell is shown in Fig. 25. In the experiments, the airspeed in the blow-down wind tunnel ranged from 0.4 to 3.0 m/s, as measured by a digital hot-wire anemometer. The turbulence intensity of the wind tunnel flow field is evaluated as 0.05-0.028 %. The wall effect can be neglected for the excuse of the blockage ratio of the ornithopter in the tunnel is less than 7.5 %. The unsteady aerodynamic forces generated from the flapping wings under the different Reynolds number were measured by a calibrated force-balance device equipped with a 6-degree of freedom load cell bought from Bertec, OH, USA. However, the present study utilizes the two degrees of freedom of the load cell where in lift as well as thrust forces can be measured simultaneously. The force specifications of 200 gf and 100 gf is used to measure the lift force along the vertical axis and the net thrust force along the horizontal axis. The net thrust force is calculated through subtracting the drag force from the thrust force. The present force gauge has a maximum error of 0.2 % of the full-scale signal due to nonlinearity or hysteresis. The data-acquisition rate of the load-cell is set as 1,000 points per second.

The authors empirically selected the air speed range from 1.5-3.0m/s for AOA of 20° and 30° during the forward flight mode and the air speed range from 0.5-1.5m/s for AOA of 60° and 70° during the hovering-like mode. Effect of increase in wind speed over lift force and net thrust force (thrust minus drag) for various AOA is shown in Fig. 26. The experiments are carried by varying the input voltage levels to the motor such as 3.0V, 3.4V and 3.7V respectively. It is observed from these experiments, for the wind speed of 1.5m/sec and an AOA of 70°, the flapping MAV experiences the maximum lift force of 14gf.

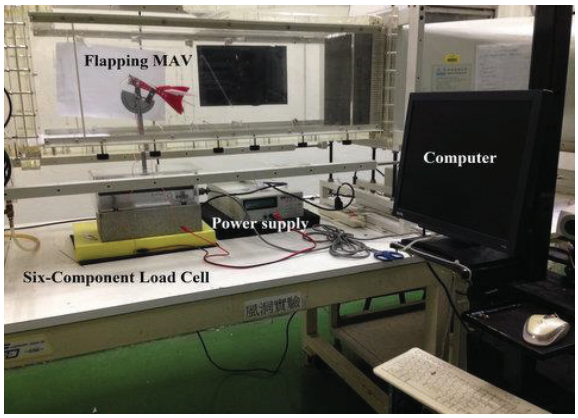

Figure 25. Wind tunnel setup with flapping MAV

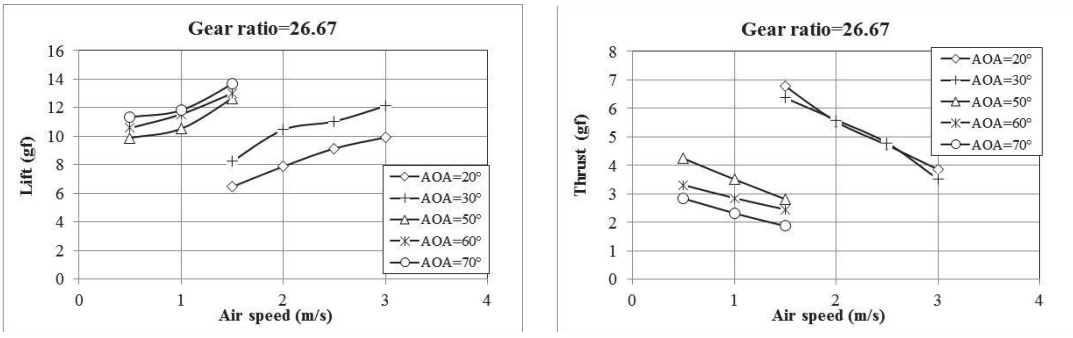

(a) (b)

Figure 26. (a) Lift and (b) Net thrust forces at different AOA, driven by 3.7 V.

(1) Effect of gear reduction ratio

The experiments are also conducted to determine the impact of gear reduction ratios on the aerodynamic performance characteristics of flapping MAV at an optimum AOA of 70°. It can be observed from the Fig. 27 that, decrease in the speed of driven gear (increase in the reduction ratio) of mechanism yields into increase in the lift as well as thrust forces. The gear reduction ratio of 26.67 has achieved the maximum lift of 13.8gf and thrust of 2.9gf in comparison to other gear reduction ratios. With the same provision of power supply, the authors believe that, the gear mechanism of 26.67 dissipates the least torque and power, and it converts the highest percentage of power to the aerodynamic forces.

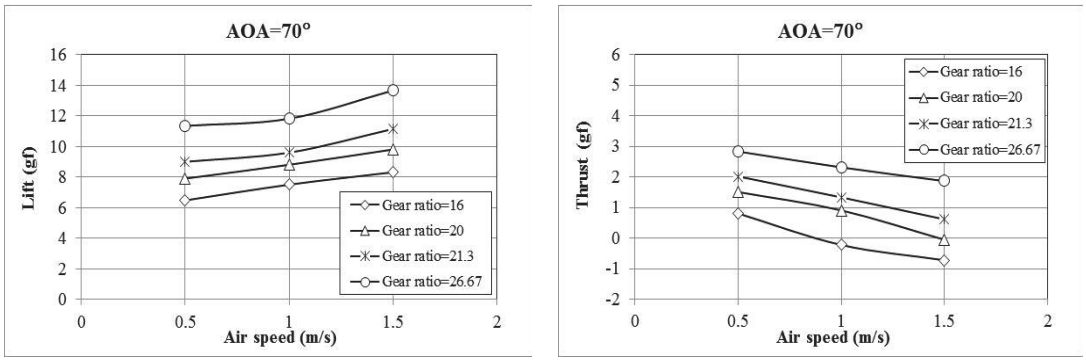

(a) (b)

Figure 27. Lift and Thrust forces at different gear reduction ratio, driven by 3.7 V.

(2) Comparison of Stephenson and Evans mechanisms

Comparison of Stephenson and Evans mechanisms on the aerodynamic performance at AOA of 20° and 60° is carried out. Experimental results show that high value of AOA yields into increase in the lift force as shown in Fig. 28. It is also observed that at AOA 20° there is a marginal difference in the lift force between Stephenson and Evans mechanisms. At 60° AOA, Evans mechanism achieves comparatively more lift than the Stephenson mechanism. Also, more drag effect is experienced in the Stephenson compared to Evans mechanism when AOA increases from 20° to 60° as shown in Fig. 29 of the net thrust force data.

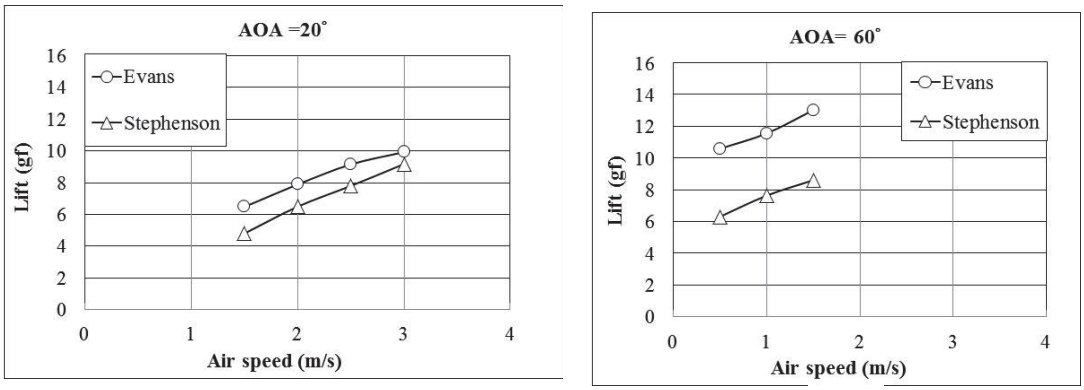

(a) (b)

Figure 28. Lift force comparison of Stephenson and Evans mechanism

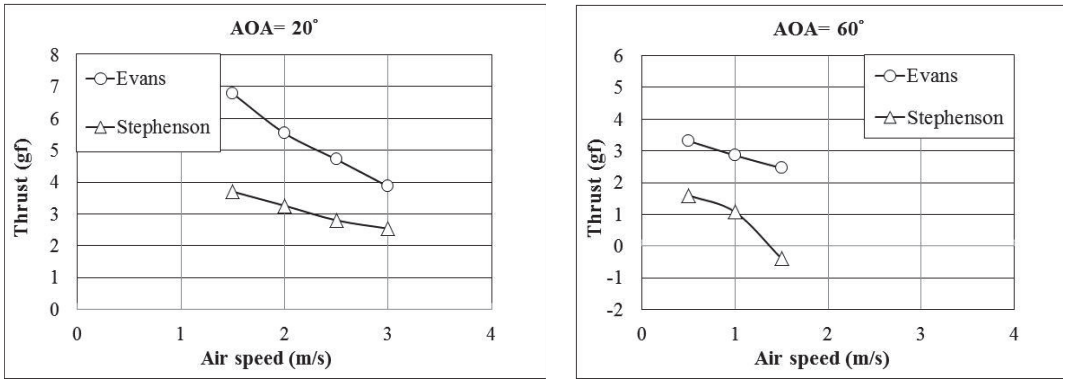

(a) (b)

Figure 29. Net thrust force comparison of Stephenson and Evans mechanism

5. CONCLUSION

Based on the iterative simulations and experimental procedures, versatile mechanisms are developed for 20 cm wing span flapping MAV with VTOL provision. Kinematic and aerodynamic performance of Stephenson and Evans mechanisms are studied in detail. Simulation studies on these mechanisms reveal that, zero phase lag is achieved with the symmetric flapping strokes. Designed mechanisms are fabricated using EDWC and injection molding techniques with adequate geometrical fidelity. Experimental studies are performed to assess the torque and aerodynamic characteristics at various AOA and wind speeds. Flapping angle of Evans mechanism is observed to be higher than that of the Stephenson mechanism. Results suggest that at an AOA 70° and gear reduction of 26.67, the flapping MAV experiences maximum lift as well as thrust. The evolved mechanisms show excellent potential for the deployment of flapping MAVs in long endurance surveillance missions that demand high transmission efficiency.

ACKNOWLEDGEMENTS

This work is supported by the Ministry of Science and Technology (MOST) of Taiwan with project numbers of 101-2632-E-032-001-MY3 and 102-2923-E-032-001-MY3 (Taiwan-side number of Indo-Taiwan Joint Project). The authors would also like to appreciate Autodesk Inc. for providing free software to students.

REFERENCES

[1] C.P. Ellington, The novel aerodynamics of insect flight: applications to micro-air-vehicles, *The Journal of Experimental Biology*, vol. 202, pp. 3439-3448, 1999.

[2] S. Ho, H. Nasseh, N. Pornsinsirirak, Y.C. Tai and C.M. Ho, Unsteady aerodynamic and flow control for flapping wing flyers, *Progress in Aerospace Science*, vol. 39, pp. 635-681, 2003.

[3] C.S. Lin, C. Hwu and W.B. Young, The thrust and lift of an ornithopter's membrane wings with simple flapping motion, *Aerospace Science and Technology*, vol. 10, pp. 111-119, 2006.

[4] L.J. Yang, C.K. Hsu, J.Y. Ho, and C.K. Feng, Flapping wings with PVDF sensors to modify the aerodynamic forces of a micro aerial vehicle, *Sensors and Actuators A: Physical*, vol. 139, pp. 95-103, 2007.

[5] B.J. Tsai and Y.C. Fu, Design and aerodynamic analysis of a flapping-wing micro air vehicle, *Aerospace Science and Technology*, vol. 13, pp. 383-392, 2009.

[6] J.H. Wu and M. Sun, Unsteady aerodynamic forces of a flapping wing, *The Journal of Experimental Biology*, vol. 207(7), pp. 1137-50, 2004.

[7] L.J. Yang, F.Y. Hsiao, W.T. Tang and I.C. Huang, 3D flapping trajectory of a micro-air-vehicle and its application to unsteady flow simulation, *International Journal of Advanced Robotic Systems*, vol. 10, paper no. 264, 2013.

[8] J.M. Miao and M.H. Ho, Effect of flexure on aerodynamic propulsive efficiency of flapping flexible airfoil, *Journal of Fluids and Structures*, vol. 22, pp. 401-419, 2006.

[9] S. Heathcote and I. Gursul, Flexible flapping airfoil propulsion at low Reynolds numbers, *AIAA Journal*, vol. 45, pp. 1066-1079, 2007.

[10] L. J. Yang, The micro-air-vehicle Golden Snitch and its figure-of-8 flapping, *Journal of Applied Science and Engineering*, vol. 15, pp. 197-212, 2012.

[11] L.J. Yang, A.F. Kuo and C.K. Hsu, Wing stiffness on light flapping micro aerial vehicles, *Journal of Aircraft*, vol. 49(2), pp. 423-431, 2012.

[12] W. Shyy, M. Berg and D. Ljungqvist, Flapping and flexible wings for biological and micro air vehicles, *Progress in Aerospace Science*, vol. 35, pp. 455-505, 1999.

[13] W. Shyy, H. Aono, S.K. Chimakurthi, P. Trizila, C.K. Kang, C.E.S. Cesnik and H. Liu, Recent progress in flapping wing aerodynamics and aeroelasticity, *Progress in Aerospace Science*, vol. 46, pp. 284-327, 2010.

[14] R. Barrett et al., Post-buckled precompressed (PBP) elements: a new class of flight control actuators enhancing high-speed autonomous VTOL MAVs, *Proceedings of SPIE - The International Society for Optical Engineering,* vol. 5762, pp. 111-122, 2005.

[15] A. Atuchin, Four wings good, two wings better- why Microraptor became extinct? *The Economist*, Nov. 10, 2012.

[16] X. Zheng et al., Hind wings in Basal birds and the evolution of leg feathers, *Science*, vol. 339, pp. 1309-1312, 2013.

[17] M. Balter, Dramatic fossils suggest early birds were biplane, *Science*, vol. 339, p. 1261, 2013.

[18] M.H. Dickinson, F.D. Lehman and S.P. Sane, Wing rotation and the aerodynamic basis of insect flight, *Science*, vol. 284, pp. 1954-1960, 1999.

[19] R. B. Srygley and A.L.R. Thomas, Unconventional lift-generating mechanisms in free-flying butterflies, *Nature*, vol. 420, pp. 660-664, 2002.

[20] S.P. Sane, The aerodynamics of insect flight, *The Journal of Experimental Biology*, vol. 26, pp. 4149-4208, 2003.

[21] L.J. Yang, C.K. Hsu, H.C. Han, and J.M. Miao, A light flapping micro-aerial-vehicle using electrical discharge wire cutting technique, *Journal of Aircraft*, vol. 46(6), pp. 1866-1874, 2009.

[22] L.J. Yang, C.Y. Kao, and C.K. Huang, Development of flapping ornithopters by precision injection molding, *Applied Mechanics and Materials*, vol. 163, pp. 125-132, 2012.

[23] U.M. Norberg: *Vertebrate Flight: Mechanics, Physiology, Morphology, Ecology and Evolution* (Springer, New York 1990).

[24] M.A.A. Fenelon and T. Furukawa, Design of an active flapping wing mechanism and a micro aerial vehicle using a rotary actuator, *Mechanism and Machine Theory*, vol. 45(2), pp. 137–146, 2010.

[25] T. Fujikawa and K. Kikuchi, Motion analysis of small flapping robot for various design and control parameters, *IEEE International Conference on Robotics and Biomimetics*, pp. 13-18, 2007.

[26] J. Ge, G. Song, J. Zhang, W. Wang, Z. Li and Y. Wang, Prototype design and performance test of an in-phase flapping wing robot, *IEEE International Symposium on Industrial Electronics (ISIE 2013)*, Taipei, Taiwan, May 2013, pp. 1- 6.

[27] C. Wang, C. Zhou, X. Zhang and C. Liu, An optimization on single-crank-double-rocker flapping wing mechanism, *2010 Fourth International Conference on Genetic and Evolutionary Computing*, Shenzhen, China, 2010, pp. 337-340.

[28] J.P. Khatait, S. Mukherjee and B. Seth, Compliant design for flapping mechanism: a minimum torque approach, *Mechanism and Machine Theory*, vol. 41 (1), pp. 3–16, 2006.

[29] J. Yan, R.J. Wood and Z.A. Agrawal and S.K. Khan, Towards flapping wing control for a micromechanical flying insect, *IEEE International Conference on Robotics and Automation*, New York, NY, 2001, pp. 3901-3908.

[30] H. Tanaka, K. Hoshino, K. Matsumoto and I. Shimoyama, Flight dynamics of a butterfly-type ornithopter, *International Conference on Intelligent Robots and Systems*,2005, pp. 2706-2711.

[31] K.M. Isaac, Force measurements on a flapping and pitching wing at low Reynolds numbers,*44th AIAA Aerospace Sciences Meeting*, Reno, NV, 2006, pp. 1-14.

[32] M. Syaifuddin, H.C. Park and N.S. Goo, Design and evaluation of a LIPCA-actuated flapping device, *Smart Materials and Structures*, vol. 15, pp. 1225-1230, 2006.

[33] B.M. Finio, B. Eum, C. Oland and R.J. Wood, Asymmetric flapping for a robotic fly using a hybrid power- control actuator, *Proceedings of the 2009 IEEE/RSJ International Conference on Intelligent Robots and Systems*, St. Louis, MO, 2009, pp. 2755-2762.

[34] T.Y. Hubel and C. Tropea, Experimental investigation of a flapping wing model, *Experiments in Fluids*, vol. 46, pp. 945-961, 2009.

[35] R.J. Wood, Design, fabrication, and analysis of a 3DOF, 3cm flapping-wing MAV, *Proceedings of the IEEE/RSJ International Conference on Intelligent Robots and Systems*, San Diego, CA, USA, Oct 29 - Nov 2, 2007, pp. 1577-1581.

[36] W. Lai, J. Yan, M. Motamed and S. Green, Force measurements on a scaled mechanical model of dragonfly in forward flight, *International Conference on Advanced Robotics*, 2005, pp. 595-600.

[37] M. Mcdonald and S.K. Agarwal, Design of a bio-inspired spherical four-bar mechanism for flapping-wing micro air-vehicle applications, *Journal of Mechanisms and Robotics*, vol. 2, pp. 021012:1-6, 2010.

[38] J.H. Park, E.P. Yang, C. Zhang and S.K. Agrawal, Kinematic design of an asymmetric in-phase flapping mechanism for MAVs, *IEEE Int. Conf. Robotics and Automation*, pp. 5099–5104, 2012.

[39] J.-S Han and J.W. Chang, Flow visualization and force measurement of an insect-based flapping wing, *48th AIAA Aerospace Sciences Meeting*, Orlando, FL, 2010, pp. 1-10.

[40] Z. E. Teoh and R. J. Wood, A Flapping-wing microrobot with a differential angle-of-attack mechanism, *IEEE International Conference on Robotics and Automation (ICRA)*, Karlsruhe, Germany, May 6-10, 2013, pp. 1381-1388.

[41] R. Madangopal, Z.A. Khan and S.K. Agrawal, Energetics-based design of small flapping-wing micro air vehicles, *IEEE/ASME Transactions on Mechatronics*, vol. 11, no. 4, pp. 433-438, 2006.

[42] C. DiLeoand X. Deng, Experimental test bed and prototype development for a dragonfly-inspired robot, *Conference on Intelligent Robots and Systems*, San Diego, CA,2007, pp. 1594-1599

[43] Z.A. Khan and S.K. Agrawal, Design and optimization of a biologically inspired flapping mechanism for flapping wing micro air vehicles, *IEEE International Conference on Robotics and Automation*, Roma, Italy, 2007, pp. 373-378

[44] S. Mukherjee and S. Sanghi, Design of a six-link mechanism for a micro air vehicle, *Defense Science Journal*, vol. 54, pp. 271-276, 2004.

[45] D. Lentink, F.T. Muijres, F. Donker-Duyvis and J.L. van Leeuwen, Vortex-wake interactions of a flapping foil that models animal swimming and flight, *The Journal of Experimental Biology*, vol. 211, pp. 267-273, 2008.

[46] S.K. Banala and S.K. Agrawal, Design and optimization of a mechanism for out-of-plane insect winglike motion with twist, *Journal of Mechanical Design/ Transactions of the ASME*, vol. 127(4), pp. 841-844, 2005.

[47] S. Avadhanula, R.J. Wood, E. Steltz, J. Yan and R.S. Fearing, Lift force improvements for the micromechanical flying insect, *IEEE International Conference on Intelligent Robotics and Systems*, Las Vegas, NV, 2003, pp. 1350-1356.

[48] R. Zbikowski, C. Galinski and C.B. Pedersen, Four-bar linkage mechanism for insectlike flapping wings in hover: concept and an outline of its realization, *Journal of Mechanical Design*, vol. 127, pp. 817-824, July 2005.

[49] T. Yokoyama, K. Tanaka and H. Ohtake, Development of a variable-wing mechanism based on flapping motion of birds, *SICE Annual Conference*, The University Electro-Communications, Japan, August 20-22, 2008, pp. 168-173.

[50] J. Yan and R. Fearing, Wing force map characterization and simulation for the micromechanical flying insect, *IEEE International Conference on Intelligent Robots and Systems*, Las Vegas, NV, 2003, pp. 1343-1349.

[51] W.J. Maybury and F.O. Lehmann, The fluid dynamics of flight control by kinematic phase lag variation between two robotic insect wings, *The Journal of Experimental Biology*, vol.207, pp. 4707-4726, 2004.

[52] S.L. Thomson et al., Experiment-based optimization of flapping wing kinematics, *47thAIAA Aerospace Sciences Meeting*, Orlando, FL, 2009, pp. 1-8.

[53] R.B. George, M.B. Colton, C.A. Mattson and S.L. Thomson, A differentially driven flapping wing mechanism for force analysis and trajectory optimization, *International Journal of Micro Air Vehicles,* vol. 4, no. 1, pp. 31-49, 2012.

[54] S. Mukherjee and R. Ganguli, Non-linear dynamic analysis of a piezoelectrically actuated flapping wing, *Journal of Intelligent Material Systems and Structures*, vol. 21, pp. 1157-1167, 2010.

[55] M.H. Hsu, H.Y. Chen, T.S. Weng and F.C. Liu, Topology structure design of 12 flapping-wing mechanisms, *Advanced Materials Research*, vols. 328-330, pp.887-891, 2011.

[56] M. Ryan, *Design optimization and classification of compliant mechanisms for flapping wing micro air vehicles*, Master Thesis, Ohio State University, USA, 2012.

[57] J.W. Gerdes, S.K. Gupta, S.A Wilkerson, A review of bird-inspired flapping wing miniature air vehicle designs, *Journal of Mechanisms and Robotics*, vol. 4, pp. 021003: 1-11, 2012.

[58] Q.T. Truong, Q.V. Nguyen, H.C. Park, D.Y. Byun and N.S. Goo, Modification of a four-bar linkage system for a higher optimal flapping frequency, *Journal of Intelligent Material Systems and Structures*, vol. 22, no. 1, pp. 59-66, 2011.

[59] Q.T. Truong, B.W. Argyoganendro and H.C. Park, Design and demonstration of insect mimicking foldable artificial wing using four-bar linkage, *Bionic Engineering*, vol. 11, no. 3, pp. 449-458, 2014

[60] V.H. Phan, P.E. Sitorus, Q.L. Phan and H.C. Park, Trailing-edge-change mechanism for longitudinal attitude control in an insect-mimicking flapping-wing system, *The 10th International Conference on Intelligent Unmanned Systems* (ICIUS'14), Sep. 29-Oct. 1, 2014, Montreal, Canada, paper no. 212.

[61] M. Keennon, K. Klingebiel, H. Won and A. Andriukov, *Development of the Nano Hummingbird: a tailless flapping wing micro air vehicle*, AIAA Paper, 2012, 0588.

[62] Information on http://www.ornithopter.org

[63] Information of Watt mechanism on the website: http://sparc.nfu.edu.tw/~cml/meeting(20070323)/9.htm

[64] E.A. Dijksman, Six-bar cognates of a Stephenson mechanism, *Journal of Mechanisms*, 6, 1970, 31-57.

[65] K. Watanabe and H. Funabashi, Kinematic analysis of Stephenson six-link mechanism, *Bulletin of JSME*, 27, 234, 1984, 2863-2870.

[66] Information of Evans mechanism on the website:www.mekanizmalar.com/evans_straight_line.html

[67] Information on http://www2.sdwfvc.cn/jpkc/jxsjjc/wljx/2/1.htm